



Impact of the Anomalous Latent Heat Flux Over the Kuroshio Extension on Western North American Rainfall in Spring: Interannual Variation and Mechanism

Jingchao Long^{1,2,3}, Chunlei Liu^{1,2,3*}, Zifeng Liu¹ and Jianjun Xu^{1,2,3}

¹South China Sea Institute of Marine Meteorology (SIMM), Guangdong Ocean University, Zhanjiang, China, ²College of Ocean and Meteorology, Guangdong Ocean University, Zhanjiang, China, ³Southern Marine Science and Engineering Guangdong Laboratory, Zhanjiang, China

OPEN ACCESS

Edited by:

Zhiwei Zhu,
Nanjing University of Information
Science and Technology, China

Reviewed by:

Bo Liu,
China University of Geosciences,
China
Lu Niu,
Alfred Wegener Institute Helmholtz
Center for Polar and Marine Research,
Germany

*Correspondence:

Chunlei Liu
liuclei@gdou.edu.cn

Specialty section:

This article was submitted to
Atmospheric Science,
a section of the journal
Frontiers in Earth Science

Received: 23 September 2020

Accepted: 23 December 2020

Published: 05 February 2021

Citation:

Long J, Liu C, Liu Z and Xu J (2021)
Impact of the Anomalous Latent Heat
Flux Over the Kuroshio Extension
on Western North American Rainfall
in Spring: Interannual
Variation and Mechanism.
Front. Earth Sci. 8:609619.
doi: 10.3389/feart.2020.609619

The Kuroshio and its extension (KE) significantly influences regional climate through meridional heat transport from the tropical ocean. In this study, the observational and reanalysis datasets are used to investigate the impact of the latent heat flux (LHF) over the KE region on downstream rainfall and the underlying mechanism. The result shows a “seesaw” structure in rainfall anomaly, dominating the Western Canada and the southwestern North America with a correlation coefficient of 0.77 between the two modes. In strong LHF years, strengthened LHF favors to enhance precipitation in the Western Canada and reduce that in the southwestern North America. This is primarily associated with an anomalous cyclonic circulation over the KE region, which enhances southwesterly precipitation and latent heating in the middle troposphere. The heating excites an anomalous cyclonic circulation to its west and an anticyclonic circulation to its east, helping to reinforce the existing anomalous cyclonic circulation in turn and form a positive feedback. The conditions associated with La Niña events favor to above processes. To the upper troposphere, the deepened anomalous cyclonic circulation due to enhanced eddy activities and atmospheric baroclinic instability over the KE strengthens subtropical westerly jet stream and thereby extends eastward on the 200 hPa level. Correspondingly, an elongated zonally lower level cyclonic circulation anomaly across the North Pacific leads to a moisture convergence in the Western Canada, which is mainly resulted from the anomalous positive vorticity advection over the left side of the exit region of the jet stream. The opposite circumstance occurs in weak LHF years, presenting an opposed anomalous circulation and rainfall pattern.

Keywords: Kuroshio and its extension, latent heat flux, western North American rainfall, ENSO, jet stream

INTRODUCTION

Sufficient water resources are extremely important for spring, the vegetation growing season (Choi and Kim, 2018), in the international agricultural center over western North America (WNA), especially the state of California (Swain et al., 2016). The precipitation over this region means the steady price of crops, food, and water security (Choi and Kim, 2018). However, California

experienced severe drought from 2012 to 2016, which causes several adverse effects to social economy and ecosystem, such as fish populations, groundwater levels, and land subsidence (Lund et al., 2018). Therefore, the improved ability to predict rainfall is needed to better optimize water resource management and prevention of disasters over this area (Guirguis et al., 2020).

In order to gain insight of the rainfall fluctuation over the WNA, many investigations in cold season (e.g., winter and spring) and warm season (e.g., summer and autumn) have been conducted. These results indicate that several atmospheric modes modulate spatial and temporal variability of precipitation from the synoptic scale to the decadal timescale (Leathers et al., 1991; Cayan et al., 1998; Dettinger et al., 1998; Seager and Hoerling, 2012; L'Heureux et al., 2015; Mundhenk et al., 2018; Guirguis et al., 2020).

On the interannual timescale, it is well known that the rainfall in the Southwest United States is influenced by large-scale forcing, such as El Niño–Southern Oscillation (Dettinger et al., 1998; Trenberth et al., 1998; Bates et al., 2001), tropical sea surface temperature (SST) variability (Seager and Hoerling, 2012), and anomalous convections (L'Heureux et al., 2015). During a typical El Niño winter or spring, a positive Pacific North America (PNA) pattern is triggered, which results in an anomalous anticyclonic circulation damping rainfall over the Northwestern United States and Western Canada, while an anomalous cyclonic circulation facilitates rainfall over the Southwestern United States (Wallace and Gutzler, 1981; Leathers et al., 1991; Cayan et al., 1998; Ault et al., 2011). Although the magnitude and extent of PNA pattern is weaker in spring than that in winter, the PNA still plays an important role in organizing the North American rainfall in spring (Horel and Wallace, 1981; Wallace and Gutzler, 1981; Leathers et al., 1991). On the other hand, the Northern Hemisphere winter and spring are also particularly dominated by the northern annular mode (NAM) or Arctic Oscillation (AO). It is a planetary-scale wave influencing the position of storm tracks and cold air activities over the WNA (Thompson and Wallace, 2000; Thompson and Wallace, 2001). In positive phase of NAM/AO, high pressure anomaly at midlatitudes favors the northward shift of the jet stream in North America, which brings wetter conditions to Alaska and reduced spring precipitation in the Western United States (McAfee and Russell, 2008).

Besides these dominant patterns including PNA and NAM/AO, the Kuroshio and its extension (KE) oceanic and atmospheric anomalies are also an important signal for climate variability over the WNA in winter and spring (Lau and Weng, 2002; Kobashi et al., 2008; Taguchi et al., 2009; Ma et al., 2015; Zhu and Li, 2016; Kuwano-Yoshida and Minobe, 2017; Zhang et al., 2017).

In the midlatitude of the North Pacific, the largest surface heat flux provided by the KE reduces near-surface static stability and enhances vertical mixing (Nonaka and Xie, 2003). In addition, the atmospheric heating aloft due to latent heat flux (Yu et al., 2015) has underlying influence on the position of the North Pacific subtropical high according to the results of Liu et al. (1999) and Wu et al. (2008) and affects the intensity and location of storm track and upper level jet stream (Taguchi et al., 2009; Zhang et al., 2017). Furthermore,

Ma et al. (2015) found that the mesoscale SST anomalies induced by oceanic eddy activity along the Kuroshio Current could strengthen the moist baroclinic instability and lead to an anticyclone anomaly over the Northeastern Pacific with reduced rainfall in winter. Over the North Pacific subtropical front region in spring, the SST front causes deep convection and modulates the atmospheric circulation anomaly by meandering of the jet stream northward in the upper troposphere (Kobashi et al., 2008). On the contrary, without SST fronts, the jet stream flows zonally and triggers downstream anomalous cyclonic circulation over the Gulf of Alaska (Kuwano-Yoshida and Minobe, 2017; Zhang et al., 2017). Those changes potentially result in atmospheric and climate remote responses (Taguchi et al., 2009; Frankignoul et al., 2010; Ma et al., 2015; Kuwano-Yoshida and Minobe, 2017). As an important quantity in air–sea interface, the LHF can well represent the exchange in water vapor and latent heat (Ding and Liu, 2001; Yu et al., 2015; Zhao et al., 2015). However, the contribution of the LHF anomaly over the KE region to the western North American rainfall variability and the physical processes related to the LHF anomaly are not understood well. Therefore, in our study, we mainly focus on the interannual variability of LHF in the KE region and its potential impact on the rainfall changes in the WNA.

The main objectives of this study are to investigate the response of atmospheric circulation and the associated western North American rainfall anomaly to the LHF anomaly in the KE region on the interannual timescale. The investigation helps to understand the linkage between the KE anomaly and the downstream rainfall variability in the WNA and its physical processes. The rest of the study is organized as following. *Data and Methods* section briefly introduces datasets and methods. *Climatology* section presents results, including climatology, interannual variability, and possible mechanisms. Concluding remarks are given in the last section.

DATA AND METHODS

Data

Several datasets are used in this study to analyze the relationship between the LHF over the Kuroshio extension and the precipitation in North America. The monthly and daily LHF data with a horizontal resolution of $1.0^\circ \times 1.0^\circ$ are from objectively analyzed air–sea flux (Yu et al., 2008). The global monthly mean precipitation data are from the Global Precipitation Climatology Project (GPCP, v2.3) (Adler et al., 2003), which combines surface and satellite observations into $2.5^\circ \times 2.5^\circ$ grid and can be obtained from 1979 to 2020. The monthly SST with horizontal resolution of $2.5^\circ \times 2.5^\circ$ is from the National Oceanic and Atmospheric Administration Extended Reconstructed SST (ERSST) version 5 (Huang et al., 2017). In addition, the reanalysis datasets are from the NCEP–DOE II monthly and daily data, including the wind, temperature, and geopotential height, at a horizontal resolution of $2.5^\circ \times 2.5^\circ$, with 17 pressure levels from 1,000 to 10 hPa. All datasets cover the period of 1980–2018.

Methods

In order to investigate the impact of LHF over the KE on the downstream rainfall on the interannual and synoptic timescale, the 9 years and 8 days running smooth are conducted for each time series. To extract the leading mode of spring LHF over the KE region, an empirical orthogonal function (EOF) analysis is conducted (Lorenz, 1956). The seasonal mean LHF in boreal spring (March, April, and May) is normalized before the EOF analysis. The coupled relationship between LHF over the KE and the North American precipitation is also investigated using the singular value decomposition (SVD) (Bretherton et al., 1992), which objectively identifies pairs of spatial patterns with maximum temporal covariance between two fields. Besides, some general methods such as correlation, linear regression, and composite analysis are employed to investigate the relationship between the atmospheric circulation anomaly and the LHF variability. For composite analysis, we chose eleven strong LHF years (1984, 1988, 1989, 1990, 1993, 1996, 2000, 2001, 2011, 2014, and 2017) and six weak LHF years (1985, 1991, 1997, 2004, 2008, and 2015) based on the criterion that the absolute value of the first principal component of LHF over the KE region (PC1) is more than 0.8 times of standard deviation away from its average. To further uncover the underlying physical processes, we diagnosed the apparent heating source, Eady maximum growth rate, and meridional heat flux due to atmospheric eddy transient.

The apparent heat source Q_1 includes the radiative heating, latent heating due to net condensation, and vertical convergence of vertical eddy transport of sensible heat (Yanai et al., 1973). Here, the inverse algorithm is employed to derive Q_1 , following the formula below (Ding and Liu, 2001):

$$Q_1 = C_p \left(\frac{p}{p_0} \right)^\kappa \left(\frac{\partial \theta}{\partial t} + V \cdot \nabla \theta + \omega \frac{\partial \theta}{\partial p} \right), \quad (1)$$

where θ denotes the potential temperature, ω the vertical velocity in the pressure coordinates, and V the horizontal wind vector. $\kappa = R/C_p$ where R is the gas constant and C_p is the specific heat capacity of the dry air. p is the pressure and p_0 equals to 1,000 hPa. The vertical integration of the Q_1 is also calculated to measure the total heat source in the atmosphere.

To understand the impact of the surface LHF on the atmospheric stratification, we diagnosed changes in linear baroclinic instability of the atmosphere, which is a source of the development of midlatitude synoptic eddy activities and storm tracks. The baroclinicity is evaluated by the maximum Eady growth rate introduced by Hoskin and Valdes (1990) and is defined as $\sigma = 0.31gN^{-1}T^{-1}|\partial T/\partial y|$, where N is the static stability parameter, T is the air temperature, and g is the gravitational acceleration. The eddy components of the meridional heat flux $v'T'$ are used as a measure of the eddy activity; the prime denotes a high-pass filter extracting the signal shorter than 8 days.

In addition, stream function was calculated by the equation, $\psi = \frac{g}{f} \cdot HGT_a$ used by Takaya and Nakamura (2001) to confirm wave-like pattern. Here, ψ is the stream function, g is the gravitational acceleration, f is the Coriolis parameter, and HGT_a is the anomalous geopotential height derived from climatology. Horizontal stationary wave activity flux was

defined by Takaya and Nakamura (2001) for demonstrating the propagation of wave energy, which is parallel to the local group velocity.

CLIMATOLOGY

In this section, climatologically averaged patterns in spring of large-scale circulation, wind, surface latent heat flux, and precipitation are briefly presented to show an overview of these factors over the North Pacific and its surrounding continents. The KE lies in the East Asian monsoon region (Wang and LinHo, 2002), where the northerly wind and southerly wind prevail in winter and summer, respectively (not shown). As shown in **Figure 1A**, with the westward extension of subtropical high in spring, the prevailing wind turns southerly, which helps to strengthen atmospheric subtropical front over the North Pacific. A rain band, corresponding to the pre-Meiyu front, extends from South China to the central of the North Pacific, with several max value cores over the KE region, implying the coupling between the oceanic front and the atmospheric front (Iizuka et al., 2013; **Figure 1B**). This rain band is also known as the atmospheric river (Zhu and Newell, 1994; Payne et al., 2020), which has a close linkage with the precipitation over the coastal region of North America. In general, with the water vapor transport by the southwesterly wind on the north side of the subtropical high, the precipitation in the Western Canada is much larger than that in the southwestern North America and Mexico (**Figure 1B**), where these are dominated by atmospheric subsidence due to subtropical high over the eastern North Pacific (**Figure 1A**). **Figure 1C** shows large interannual variability of latent heat flux over the KE region and corresponding precipitation variability, implying a potential influence on regional and even remote climate variations deduced by the study of Zhu and Li (2016).

INTERANNUAL VARIABILITY

Leading Mode of LHF over the KE Region

The EOF analysis is used to separate spring LHF anomaly over the KE region into different spatial modes that have various variability features. As shown in **Figure 2A**, the first EOF mode shows a spatial uniform LHF anomaly along the Kuroshio pathway with prominent interannual variability (PC1), which accounts for 30.35% of the total variance. While the second mode (PC2) presents a northwest–southeast contrast distribution of LHF anomaly, accounting for additional 14.41% (**Figure 2B**). The leading mode pattern is similar to the distribution of climatology and standard deviation of LHF (**Figures 1B,C**). In order to represent the primary information of LHF interannual variability, the normalized PC1 time series (**Figure 2C**) is defined as an indicator for the variability of LHF over the KE region and used in the following discussion (Yu et al., 2015).

To estimate the relationship between the PC1 and the precipitation, the map of the correlation coefficient between them is shown in **Figure 3**. Three zonally elongated bands of

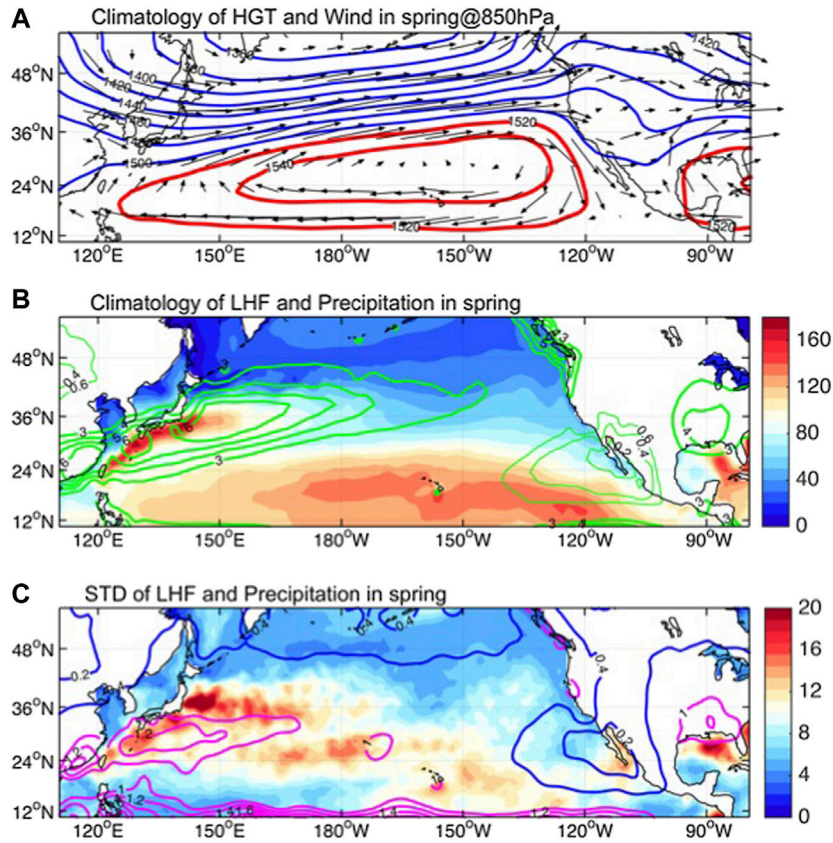


FIGURE 1 | (A) Climatology of spring geopotential height (HGT, contours, gpm) and horizontal wind (vector, m/s) at 850 hPa, **(B)** climatology of spring latent heat flux (shading, W/m²) and precipitation (contours, mm/day), **(C)** standard deviation of latent heat flux (shading, W/m²), and precipitation (contours, mm/day).

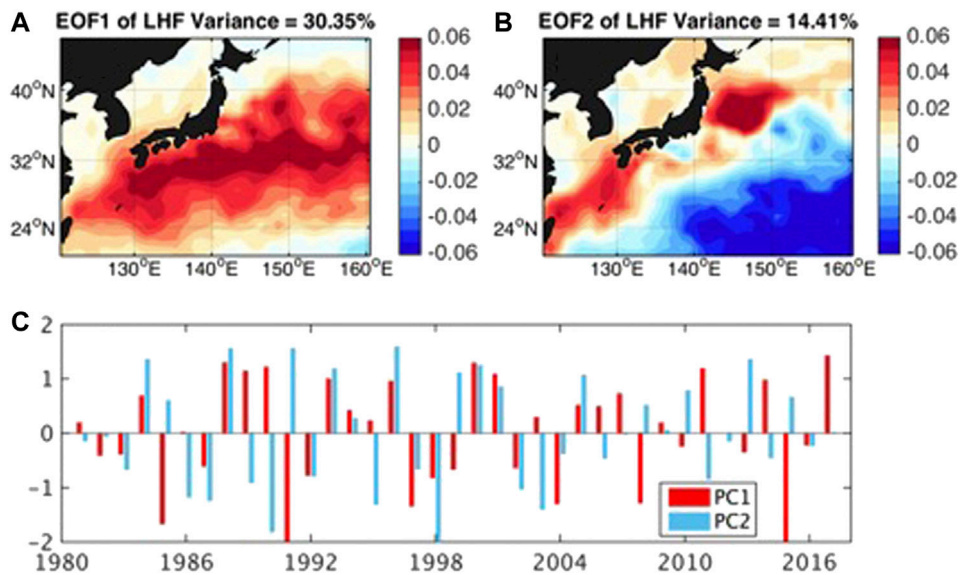
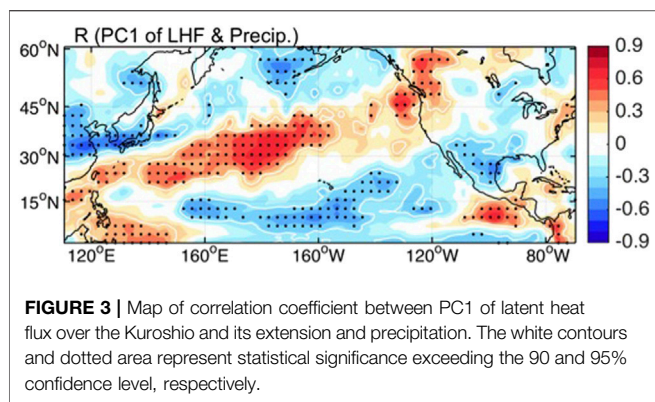
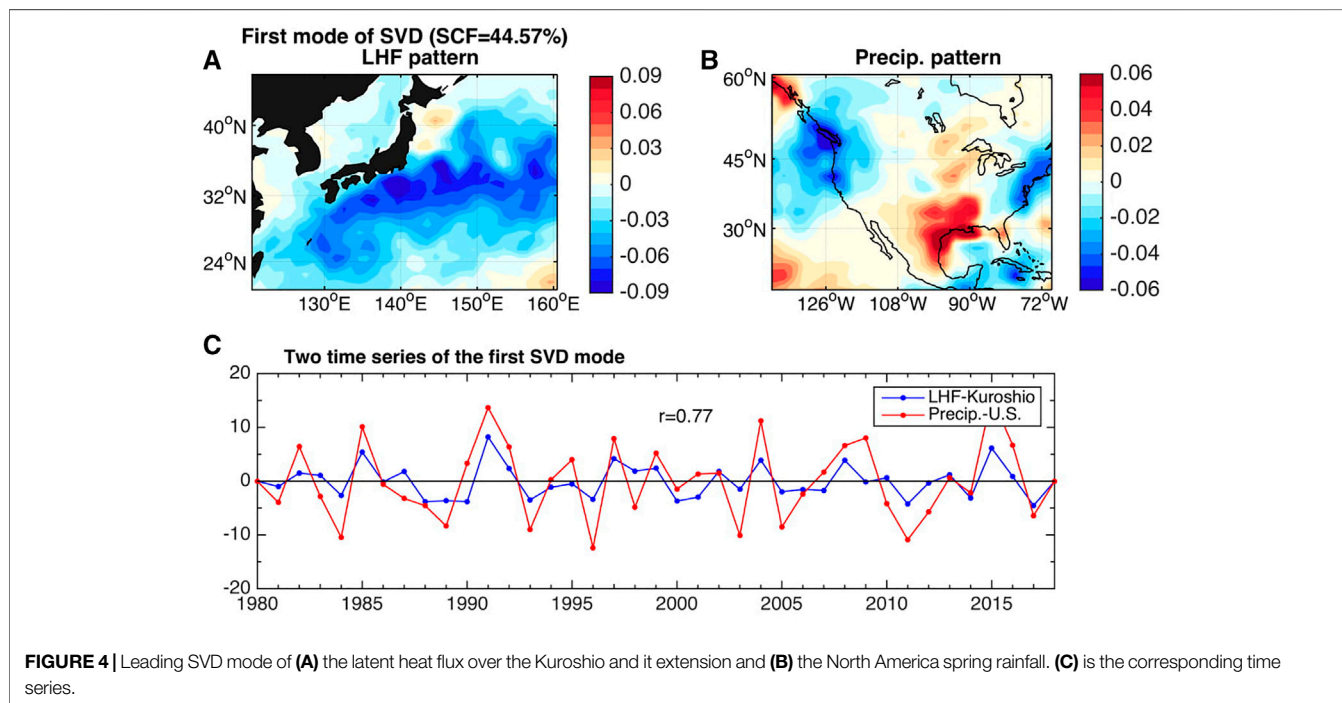


FIGURE 2 | (A) Spatial pattern of the first EOF mode of latent heat flux over the Kuroshio and its extension for the period of 1980–2018, and **(B)** is same as **(A)**, but for the second EOF mode. **(C)** Normalized the first (red bar) and the second (blue bar) principal component of latent heat flux over the Kuroshio and its extension.



the total variance. Both LHF over the KE region and spring rainfall in the leading SVD display a coherent interannual variability with correlation coefficient of 0.77 between the two time series (**Figure 4C**). An uniform pattern of the LHF mode (**Figure 4A**) is consistent with the first EOF mode of LHF over the KE region, while the North American rainfall pattern (**Figure 4B**) is similar to the second EOF mode of spring rainfall with a positive (negative) precipitation core over the coastal region of Western Canada and a negative (positive) core over the southern North America around the Gulf of Mexico (not shown). The leading SVD mode illustrates that the spring North American rainfall dipole mode is really tightly coupled with the LHF mode over the KE region. Therefore, our question is that what



correlation coefficient pass through the North Pacific to the coast of North America, where the correlation coefficient is significant again. This pattern presents a seesaw structure in precipitation anomaly between the southwestern North America and the Western Canada, at a high correlation with LHF anomaly over the KE region. In addition, the maximum correlation coefficient area is downstream to the central Pacific with the center at 180°E and 30°N, implying a prominently local atmospheric response to the LHF release in the KE region.

Coupled Relationship Between LHF Variability and Rainfall Pattern in North America

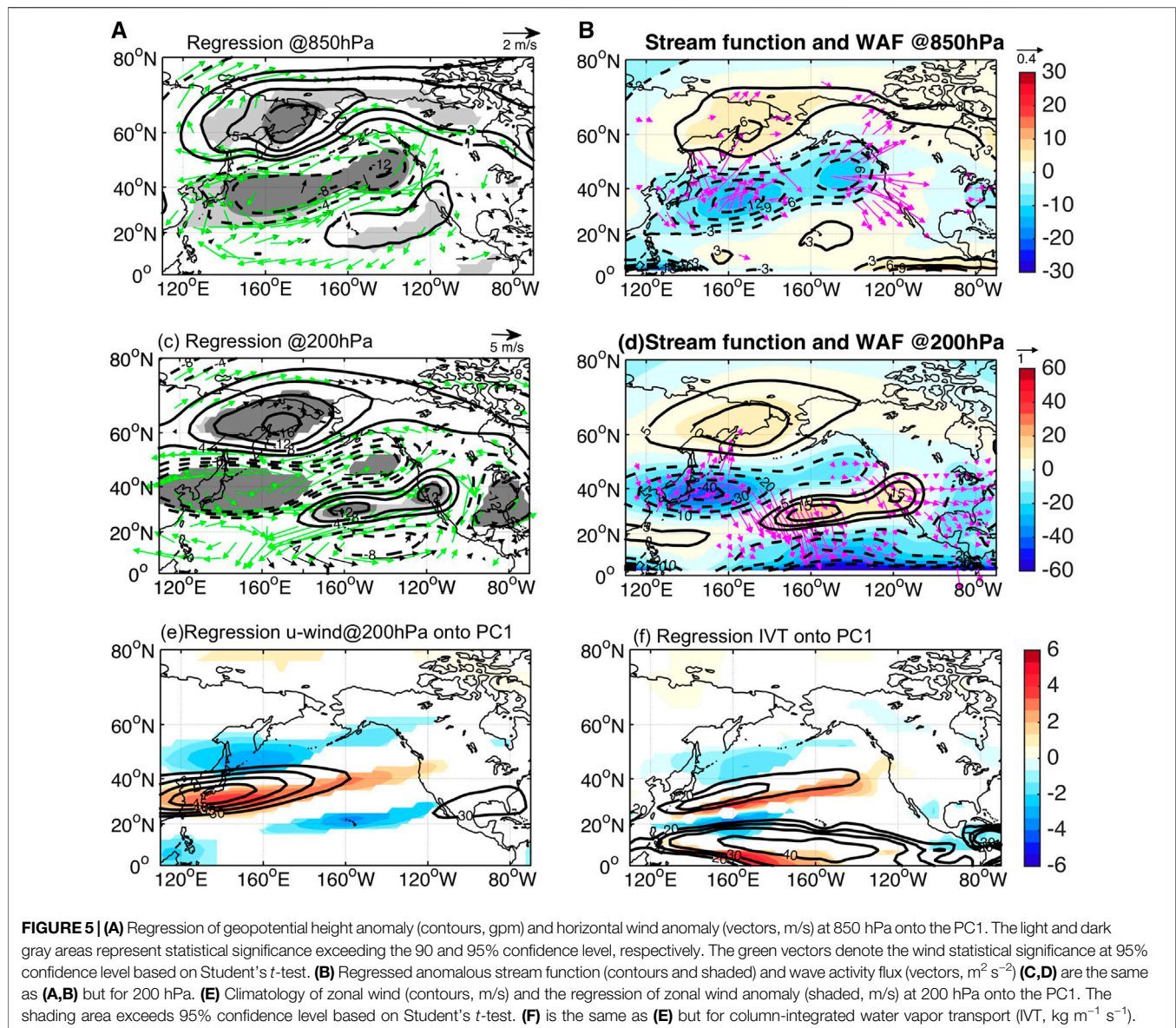
To validate the result of correlation analysis, the coupled modes between the spring LHF over the KE region and the North American rainfall are obtained by employing an SVD analysis. As shown in **Figure 4**, this coupled mode accounts for 44.57% of

mechanism links the LHF variation over the KE region and the spring rainfall anomaly in North America?

POSSIBLE LINKAGE MECHANISMS

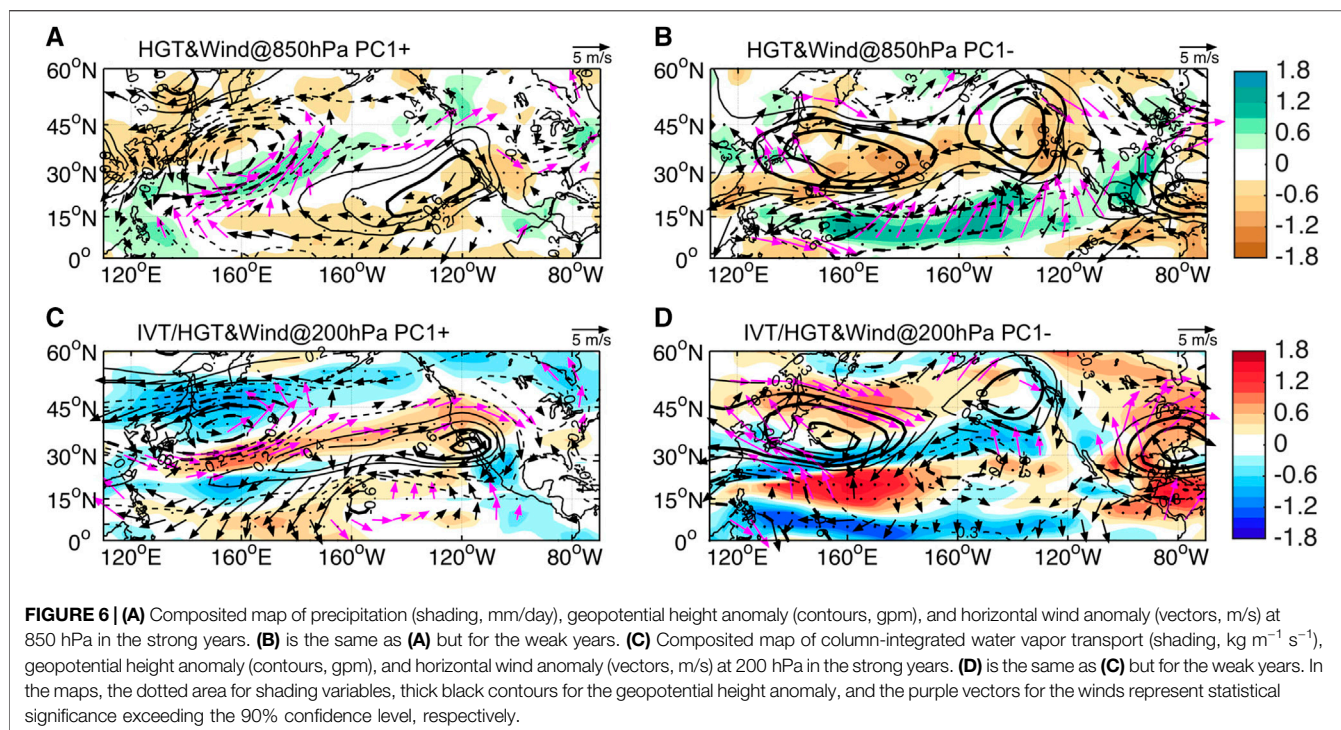
Associated Circulation Anomaly of LHF PC1

To analyze the anomalous circulation that influences the North American precipitation, the anomalous geopotential height, horizontal wind (**Figures 5A,C**), upper level jet stream (**Figure 5E**), and column-integrated water vapor transport (**Figure 5F**) are regressed onto PC1 of LHF over the KE region. The corresponding anomalous stream function and wave activity flux (WAF) are also calculated to diagnose the Rossby wave energy propagation (**Figures 5B,D**). Apparently, the dipole structure of the North American rainfall is tightly related to the zonally elongated cyclonic (anticyclonic) circulation anomaly extending from the North Pacific to the WNA



(Figures 5A,C). Furthermore, the changes of LHF over the KE region seem to be an energy source that maintains the anomalous barotropic cyclonic (anticyclonic) circulation (Figures 5B,D). Figure 5B shows an enhanced anomalous cyclonic circulation and WAF at 850 hPa over the northeastern Pacific, which is probably associated with the condensational heating due to strengthened precipitation (Figure 3). In Figure 5D, an evident feature is the WAF at 200 hPa southeastward propagates in two pathways, which are relatively independent from each other. The one pathway is from the KE region to the anticyclonic anomaly over the subtropical central Pacific, and another one is along the coast of the WNA (east side of subtropical high) from the north to south. Remarkably, the WAF propagates eastward continuously, which might have a profound influence on the precipitation in the Eastern United States.

As shown in Figure 5E, the regressed zonal wind anomaly at 200 hPa is corresponding to the anomalous circulation in Figure 5C, indicating that the enhanced LHF over the KE region helps the subtropical upper level jet stream strengthen and extend eastward to the coast of North America. This change probably modulates low-level circulation and precipitation anomaly, which will be discussed in *Climatology* section. This result is similar to the response of the upper level jet stream on the subtropical oceanic front in spring (Zhang et al., 2017), yet some differences exist from the forcing of the oceanic front and mesoscale eddies in winter due to the difference in the forcing region and distinct seasonal background (Ma et al., 2015; Kuwano-Yoshida and Minobe, 2017). The linear response of the water vapor transport is also estimated by regressing the column-integrated water vapor transport (Payne et al., 2020) onto PC1. Figure 5F illustrates that more water vapor transport in the



west coast of Canada depends on the enhanced southwesterly wind from the lower level to the upper level (Figures 5A,C), which is conducive to the increase of precipitation there.

Asymmetrical Response of Atmospheric Circulation on LHF Anomaly

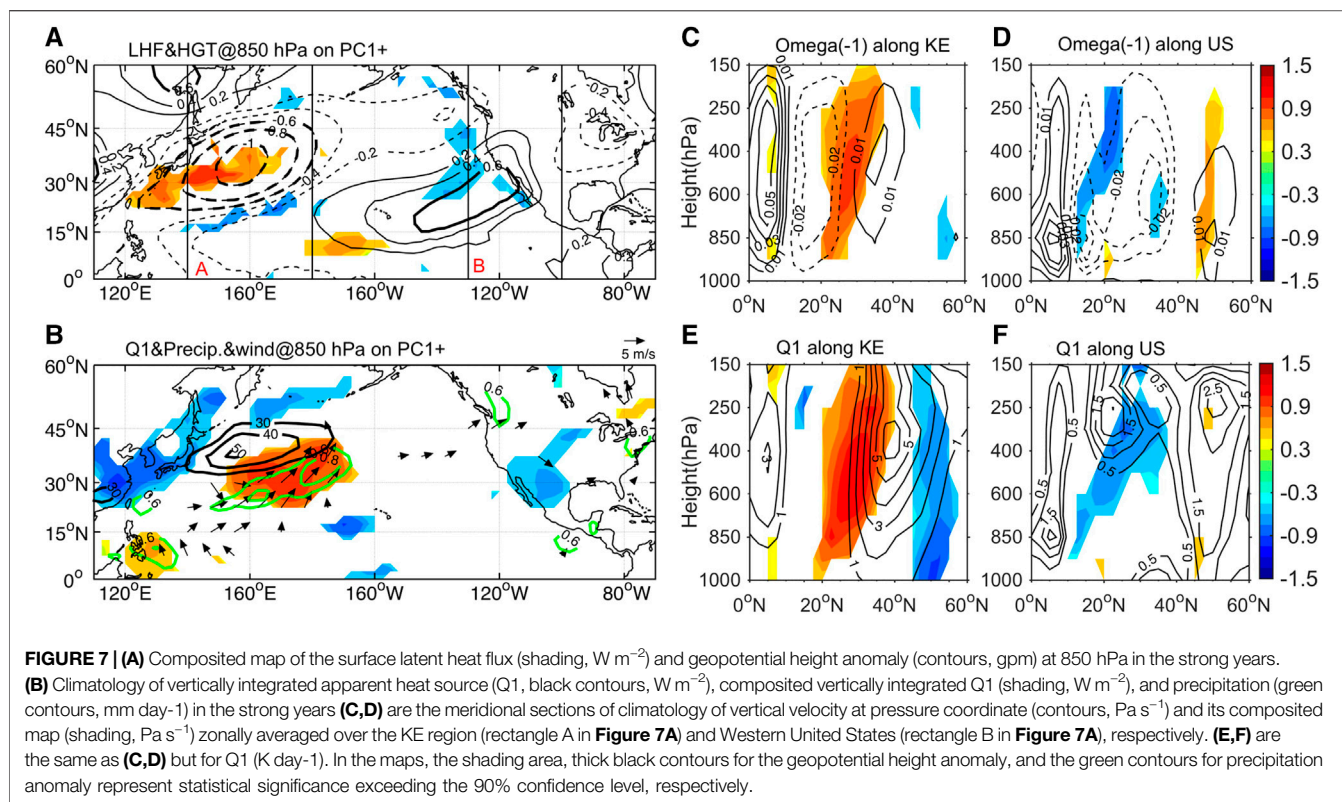
To analyze the mechanism of the LHF anomaly influence over the KE region on the western North American rainfall on the interannual timescale, Figure 6 shows the composite map of MAM-averaged geopotential height, horizontal winds at 850 hPa with precipitation, and those at 200 hPa with IVT based on eleven strong and six weak LHF years as defined in *Data and Methods* section. The composite maps indicate an asymmetrical response of the atmosphere to the KE LHF forcing.

With regard to the composite of strong years, an equivalent barotropic dipole structure of atmospheric circulation dominates the North Pacific (Figures 6A,C). The cyclonic circulation anomaly exists over the KE region and is zonally elongated to the Western Canada, accompanied with the strengthened southerly wind, providing much more water vapor for precipitation. Simultaneously, an anticyclonic circulation anomaly imposed on the subtropical high lies on the southeast of the North Pacific, damping the precipitation in the southwestern North America and Mexico (Figure 6A). Conversely, in the weak years, the cyclonic circulation generated in strong years is replaced by a seemingly continuous anticyclonic circulations, which causes anomalous weak water vapor transport (Figure 6D) to the coast of Western United States and increases precipitation around the Gulf of Mexico (Figure 6B). It is evident that the

intensity of anomalous circulations near the coast of western North America is asymmetric.

Impact of Strengthened Heating on Lower Level Circulation

To answer the question how the variability of LHF over the KE region influences the rainfall changes in the WNA, we take insight into the circumstance in strong years. Figure 7A,B shows that with the increase of LHF, the anomalous low forms aloft due to reducing near-surface static stability and enhancing vertical mixing (Nonaka and Xie, 2003). Correspondingly, the enhanced southwesterly wind transports more water vapor and strengthens precipitation over the southeast of the low anomaly (Figure 6A). The apparent heat source (Q_1) anomaly due to condensational heating with the maximum in mid-troposphere (Figure 7E) can trigger anomalous southerly wind at the bottom of the maximum heat source and anomalous northerly wind above that (Liu et al., 1999; Wu et al., 2008), accompanying with strong ascending motion (Figure 7C). As shown in Figure 7E, it is clear that the anomalous maximum center of the heat source is located at 400 hPa, which is lower than the heating anomaly associated with the subtropical SST front (Zhang et al., 2017). According to the theory proposed by previous work (Liu et al., 1999; Wu et al., 1999), positive $\partial Q_1 / \partial z$ facilitates to excite an anomalous cyclonic circulation to its west and an anomalous anticyclonic circulation to its east due to the anomalous southerly wind. Strengthened cyclonic circulation induced by the latent heating can also reinforce the existing cyclonic circulation anomaly, which can be regarded as a positive feedback. Note that the response of the dipole circulation is confined in low-middle troposphere due to the maximum center of the



heat source at 400 hPa. In western North America (zonally averaged over region B in **Figure 7A**), the enhanced Q_1 in **Figure 7F** (upward motion in **Figure 7D**) around 50°N in Western Canada, and suppressed Q_1 (descending motion) around 25°N over the coast of the WNA confirm the rainfall change associated with the anomalous circulation. The anomalous rainfall and atmospheric heating over the coastal region of the WNA probably affect the rainfall anomaly over the Eastern United States *via* wave energy dispersion at the upper level from the west to east of United States (**Figure 5D**).

Impact of Shift of Upper Level Jet Stream on Lower Level Circulation

In order to investigate the formation of equivalent barotropic circulation anomaly from low–middle level to upper troposphere, we diagnostic relevant physical processes shown in **Figure 8**.

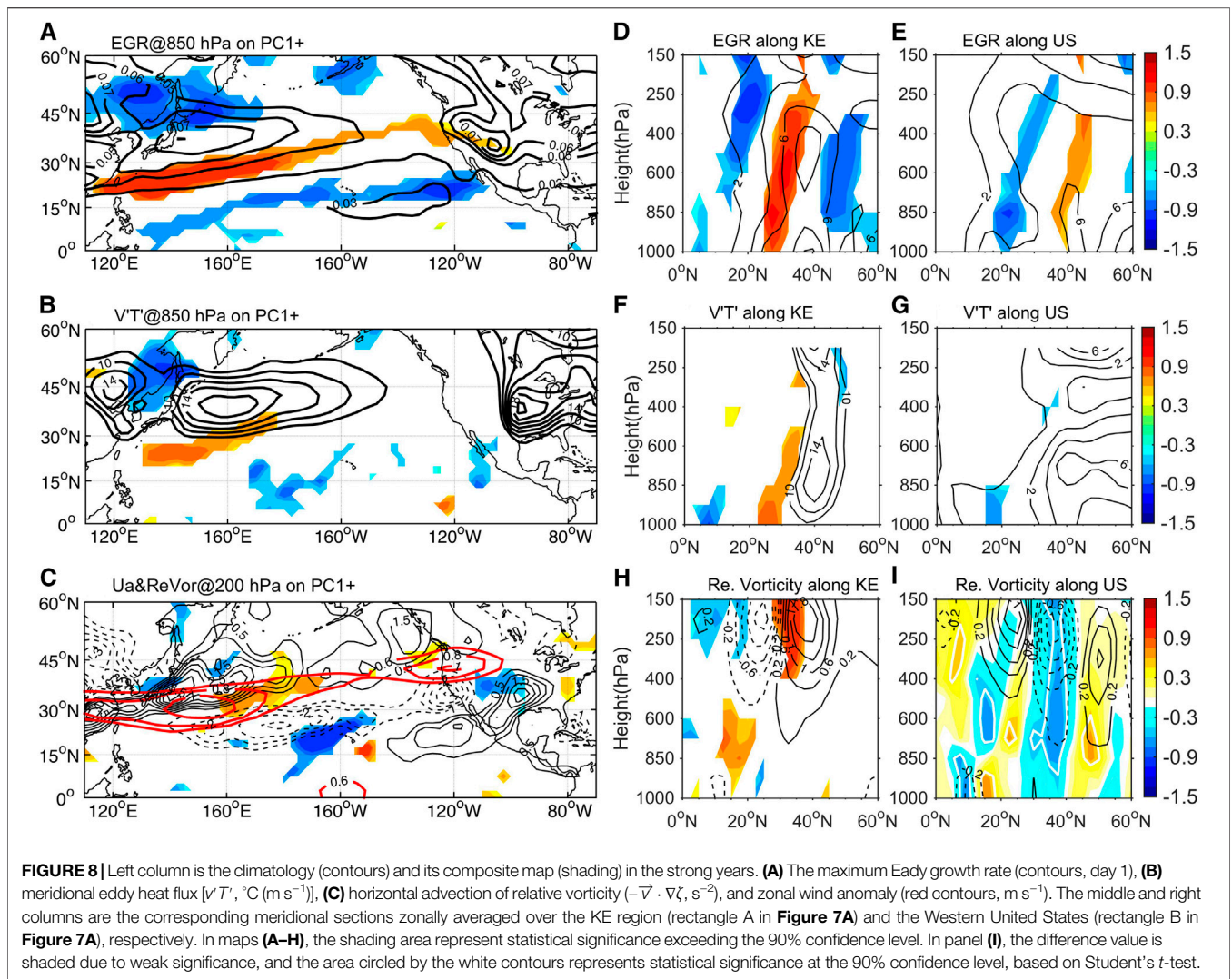
As shown in **Figure 8A**, the climatology of Eady growth rate denotes that the atmospheric front lies on the KE region and a zonally elongated band structure of the anomalous Eady growth rate to the south flank. The vertical structure in **Figure 8D** indicates a larger Eady growth rate value in the lower troposphere, which implies that the synoptic activities are easy to develop (Simmons and Hoskins, 1978). The strengthened baroclinic instability extends from near the surface to the upper troposphere with a northward tilt with height, suggesting that the atmospheric front is coupled with the KE SST front (Iizuka et al., 2013; Moteki and Manda, 2013). Furthermore, the synoptic scale transient eddy activities are also measured by the meridional eddy heat flux ($v'T'$) (Blackmon et al., 1977), in which v'

and T' are 8-day high-pass filtered v-component of the wind and air temperature, respectively (**Figure 8B**). **Figure 8B,F** indicates that the strong LHF strengthens meridional eddy heat flux over the KE region. Although eddy heat flux is not evident in the western North America (**Figure 8G**), the enhanced Eady growth rate illustrates that strong LHF favors to develop synoptic disturbance and convection (**Figure 8E**).

The increase of baroclinic eddy activities, which trap more available potential energy, is likely to produce more eddy kinetic energy and deepen the anomalous cyclonic circulation over the KE region, which further strengthen zonal wind from the lower troposphere to upper level (Gan and Wu, 2015). **Figure 8C,H** suggests that the upper level jet stream represented by zonal wind speed at 200 hPa is enhanced and extended to the western North America. The enhanced jet stream modulates the large-scale circulation (Kuwano-Yoshida and Minobe, 2017). For instance, the cyclonic circulation anomaly over the Western Canada is strengthened because of the increased positive relative vorticity advection to the north of the jet stream (**Figure 8C**), which extends across the troposphere, helping the development of low-level cyclonic circulation (**Figure 8I**).

Role of La Niña in the Anomalous Precipitation over the WNA

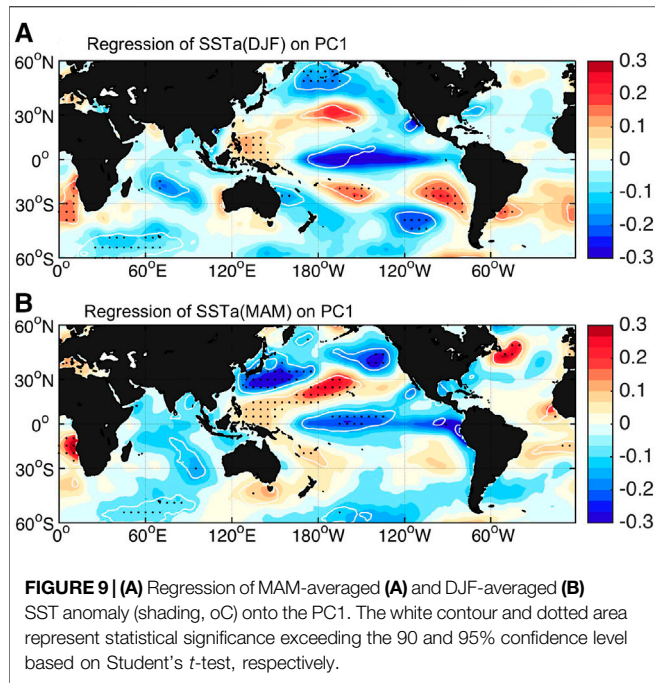
Since the tropical SST variability has a pronounced impact on both oceanic current and atmospheric circulation in the North Pacific, such as a strong response of the Kuroshio to ENSO (Mei et al., 2006) and the formation of the PNA teleconnection (Wallace and Gutzler, 1981).



In order to investigate the relationship between tropical SST variability and the LHF over the KE region, the following spring (MAM) and previous winter (DJF) SST anomaly are regressed onto PC1. **Figure 9A** displays that the intensity of LHF over the KE region in the following spring is related with a strong negative SST anomaly over the central Pacific at the previous DJF, namely, a La Niña-like pattern. However, this relationship does not exceed the 95% confidence level, implying that the impact of La Niña-like pattern in previous winter on the spring LHF over the KE region is not prominent. During MAM (**Figure 9B**), although the cold SST anomaly over the central Pacific weakens, the area with statistical significance exceeding the 95% confidence level is extended. Meanwhile, the local SST over the KE region is strengthened, suggesting the response of local SST to the LHF release due to frequent cold air southward intruding over the KE region (**Figure 10A**).

In order to investigate the impact of ENSO on western North American rainfall and its different role compared with that by the Kuroshio LHF anomaly, **Figure 10** presents the composite

anomalies based on the criterion that the absolute value of the Niño 3.4 index in MAM is more than 0.8 times of standard deviation away from its average. For composite analysis, eight typical La Niña years (1981, 1984, 1985, 1989, 1999, 2000, 2008, and 2011) and seven typical El Niño years (1983, 1987, 1992, 1993, 1998, 2015, and 2016) are employed. **Figure 10A** shows that no significant less precipitation over the southwestern North America and more precipitation over the Western Canada in spring, since the anomalous high lain at the west of coastal California is relatively weak and shrunken on the ocean. Actually, the anomalous anticyclonic circulation in **Figure 6A** is from the combination of the Kuroshio LHF forcing and La Niña effect. On the one hand, the anomalous high over the subtropical eastern Pacific induced by La Niña helps to strengthen and extend the high anomaly eastward, damping precipitation over the southwest of North America (**Figure 6A**). On the other hand, anomalous low precipitation over the western Pacific facilitates to cold air outbreak from the Asian continent in spring of La Niña years (Li and Mu, 2000;

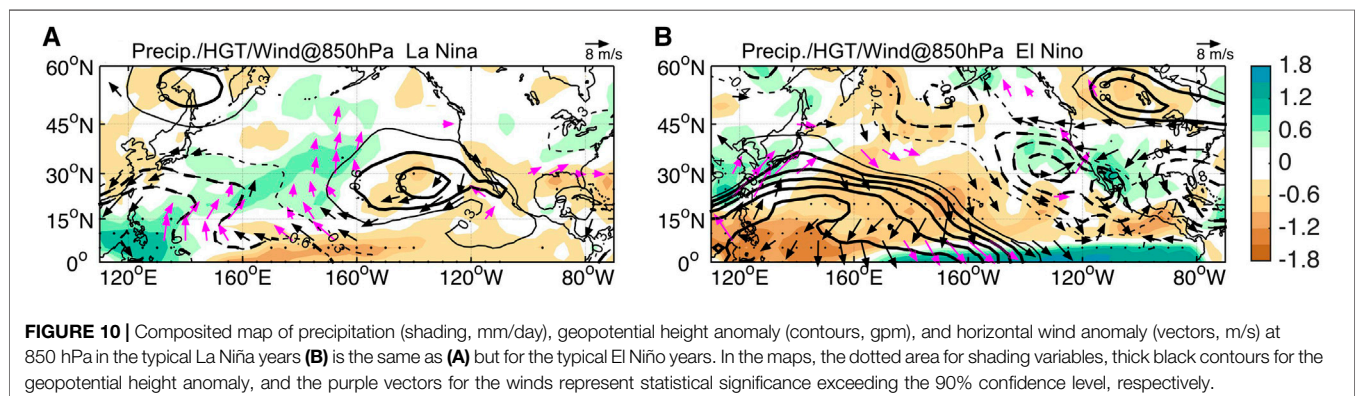


Zhun and Chen, 2002; Kim et al., 2014) and enhances LHF release. In following spring of El Niño years, an anomalous low over the eastern subtropical Pacific (**Figure 10B**) favors more rainfall in the Southwest United States and Mexico, which acts similar role in the weak LHF years (**Figure 6B**).

SUMMARY AND DISCUSSION

The Kuroshio transports a large amount of heat from the tropics to the midlatitudes (Zhang et al., 2012), influencing the regional and hemispheric climate (Minobe et al., 2008; Hu et al., 2015). In this study, the observational data and reanalysis data are employed to investigate the impact of the LHF over the KE region on downstream rainfall and its underlying mechanisms.

An empirical orthogonal function (EOF) analysis is conducted to extract the leading mode and the first principal component of spring LHF over the KE (Lorenz, 1956). And then, we diagnose the relationship between LHF anomaly over the KE region and the western North American rainfall variability through correlation analysis and singular value decomposition (SVD). The result shows a “seesaw” structure in rainfall anomaly, dominating the Western Canada and the southwestern North America with correlation coefficient of 0.77 between the two modes (**Figures 3, 4**). Taking insight into the mechanism of this phenomenon, we found that in strong years, the strengthened LHF releases favors to enhance precipitation in the Western Canada and reduce that in the southwestern North America. This is primarily associated with an anomalous cyclonic circulation over the KE region due to the strong LHF, which enhances the southwesterly, precipitation, and latent heating in the middle troposphere. The heating excites an anomalous anticyclonic circulation to its east and an anomalous cyclonic circulation to its west, which helps to reinforce the existing anomalous anticyclonic circulation in turn and form a positive feedback (**Figures 6A, 7A**; Liu et al., 1999; Wu et al., 1999). In addition, the anomalous anticyclonic circulation over the subtropical eastern North Pacific induced by La Niña events enhances southerly wind in the west flank and strengthens the feedback mentioned above. On the other hand, because strong LHF is conducive to eddy activities and the strengthening of the atmospheric baroclinic instability over the KE, the enhanced and deepened anomalous cyclonic circulation in troposphere strengthens subtropical westerly jet and thereby extends eastward on the 200 hPa level. Correspondingly, a zonally elongated lower level cyclonic circulation anomaly across the North Pacific leads to a moisture convergence in the Western Canada, which is mainly resulted from the anomalous positive vorticity advection over the left side of the exit region of the jet stream (**Figure 8C**). On the contrary, the southwestern North America is located at the right side of the exit region of the jet axis, which is not conducive to the vertical convection and rainfall (**Figure 8I**). In weak LHF years, an asymmetrical anomalous circulation and rainfall



patterns are presented, which is probably associated with asymmetry of ENSO effect and the influence from mid-high latitude.

DATA AVAILABILITY STATEMENT

The original contributions presented in the study are included in the article/Supplementary Material, further inquiries can be directed to the corresponding author.

AUTHOR CONTRIBUTIONS

The contribution of JL: proposing original idea, data analysis, figures preparation, and manuscript writing; the contribution of CL: proposing original idea and improving manuscript; the contribution of ZL: preparing a part of figures and data analysis; the contribution of JX: data analysis and improving manuscript.

REFERENCES

- Adler, R. F., Huffman, G. J., Chang, A., Ferraro, R., Xie, P.-P., Janowiak, J., et al. (2003). The version-2 global precipitation climatology project (GPCP) monthly precipitation analysis (1979–Present). *J. Hydrometeorol.* 4, 1147–1167. doi:10.1175/1525-7541(2003)004<1147:TVGPCP>2.0.CO;2
- Ault, T. R., Macalady, A. K., Pederson, G. T., Betancourt, J. L., and Schwartz, M. D. (2011). Northern hemisphere modes of variability and the timing of spring in western North America. *J. Clim.* 24 (15), 4003–4014. doi:10.1175/2011JCLI4069.1
- Bates, G. T., Hoerling, M. P., and Kumar, A. (2001). Central U.S. springtime precipitation extremes: teleconnections and relationships with sea surface temperature. *J. Clim.* 14 (17), 3751–3766. doi:10.1175/1520-0442(2001)0142.0.CO;2
- Blackmon, M. L., Wallace, J. M., Lau, N. C., and Mullen, S. L. (1977). An observational study of the northern hemisphere wintertime circulation. *J. Atmos. Sci.* 34, 1040–1053. doi:10.1175/1520-0469(1977)034<1040:AOSOTN>2.0.CO;2
- Bretherton, C. S., Smith, C., and Wallace, J. M. (1992). An intercomparison of methods for finding coupled patterns in climate data. *J. Clim.* 5, 541–560. doi:10.1175/1520-0442(1992)005<0541:AIOMFF>2.0.CO;2
- Cayan, D. R., Dettinger, M. D., Diaz, H. F., and Graham, N. E. (1998). Decadal variability of precipitation over western North America. *J. Clim.* 11 (12), 3148–3166. doi:10.1175/1520-0442(1998)0112.0.CO;2
- Choi, W., and Kim, K. Y. (2018). Physical mechanism of spring and early summer drought over North America associated with the boreal warming. *Sci. Rep.* 8 (1), 7533. doi:10.1038/s41598-018-25932-5
- Dettinger, M. D., Cayan, D. R., Diaz, H. F., and Meko, D. M. (1998). North–south precipitation patterns in western North America on interannual-to-decadal timescales. *J. Clim.* 11, 3095–3111. doi:10.1175/1520-0442(1998)011<3095:NSPPIW>2.0.CO;2
- Ding, Y. H., and Liu, Y. J. (2001). Onset and the evolution of the summer monsoon over the South China Sea during SCSMEX field experiment in 1998. *J. Meteor. Soc. Japan Ser. II* 79 (1B), 255–276. doi:10.2151/jmsj.79.255
- Frankignoul, C., Sennéchal, N., Kwon, Y. O., and Alexander, M. A. (2011). Influence of the meridional shifts of the kuroshio and the oyashio extensions on the atmospheric circulation. *J. Clim.* 24 (3) 762–777. doi:10.1175/2010JCLI3731.1
- Gan, B., and Wu, L. (2015). Feedbacks of sea surface temperature to wintertime storm tracks in the north atlantic. *J. Clim.* 28 (1) 306–323. doi:10.1175/JCLI-D-13-00719.1

FUNDING

We declare all sources of funding received for the research being submitted. This study has been jointly supported by the National Natural Science Foundation of China (Grant No. 42075036 and 41905006), the National Key R&D Program of China (Grant No. 2018YFC1505902).

ACKNOWLEDGMENTS

We appreciate the data resources providers. The OAflux data was downloaded from ftp://ftp.who.edu/pub/science/oaflux/data_v3. The GPCP, v2.3 was downloaded from <https://www.psl.noaa.gov/data/gridded/data.gpcp.html>. The ERSST version5 was downloaded from <http://www.esrl.noaa.gov/psd/data/gridded/data.noaa.ersst.v5.html>. And the NCEP-DOE II monthly data was downloaded from <https://www.psl.noaa.gov/data/gridded/data.ncep.reanalysis2.html>.

- Guirguis, K., Gershunov, A., De Florio, M. J., Shulgina, T., Delle Monache, L., Subramanian, A. C., et al. (2020). Four atmospheric circulation regimes over the North Pacific and their relationship to California precipitation on daily to seasonal timescales. *Geophys. Res. Lett.* 47, e2020GL087609. doi:10.1029/2020GL087609
- Horel, J. D., and Wallace, J. M. (1981). Planetary-scale atmospheric phenomena associated with the southern oscillation. *Mon. Weather Rev.* 109, 813–829. doi:10.1175/1520-0493(1981)109,0813:PSAPAW.2.0.CO;2
- Hoskins, B. J., and Valdes, P. J. (1990). On the existence of storm tracks. *J. Atmos. Sci.* 47 (15), 1854–1864. doi:10.1175/1520-0469(1990)047<1854:OTEOST>2.0.CO;2
- Hu, D., Wu, L., Cai, W., Gupta, A. S., Ganachaud, A., and Qiu, B., et al. (2015). Pacific western boundary currents and their roles in climate. *Nature* 522 (7556), 299. doi:10.1038/nature14504
- Huang, B., Thorne, P. W., Banzon, V. F., Boyer, T., and Zhang, H. M. (2017). Extended reconstructed sea surface temperature version 5 (ERSSTv5), upgrades, validations, and intercomparisons. *J. Clim.* 30 (20), 8179–8205. doi:10.1175/JCLI-D-16-0836.1
- Iizuka, S., Shiota, M., Kawamura, R., and Hatsushika, H. (2013). Influence of the monsoon variability and sea surface temperature front on the explosive cyclone activity in the vicinity of Japan during northern winter. *SOLA* 9, 1–4. doi:10.2151/sola.2013-001
- Lund, J., Medellín-Azuara, J., Durand, J. R., and Stone, K. (2018). Lessons from California’s 2012–2016 drought. *J. Water Resour. Plann. Manag.* 144 (10), 04018067. doi:10.1061/(ASCE)WR.1943-5452.0000984
- Kim, J.-W., Yeh, S.-W., and Chang, E.-C. (2014). Combined effect of El Niño-southern oscillation and pacific decadal oscillation on the East Asian winter monsoon. *Clim. Dynam.* 42, 957–971. doi:10.1007/s00382-013-1730-z
- Kobashi, F., Xie, S. P., Iwasaka, N., and Sakamoto, T. T. (2008). Deep atmospheric response to the north pacific oceanic subtropical front in spring. *J. Clim.* 21 (22), 5960–5975. doi:10.1175/2008JCLI2311.1
- Kuwano-Yoshida, A., and Minobe, S. (2017). Storm-track response to SST fronts in the northwestern Pacific region in an AGCM. *J. Clim.* 30, 1081–1102. doi:10.1175/JCLI-D-16-0331.1
- Lau, W. K. M., and Weng, H. (2002). Recurrent teleconnection patterns linking summertime precipitation variability over East Asia and North America. *J. Meteor. Soc. Japan* 80 (6), 1309–1324. doi:10.2151/jmsj.80.1309
- Leathers, D. J., Yarnal, B., and Palecki, M. A. (1991). The Pacific/North American teleconnection pattern and United States climate. Part I: regional temperature and precipitation associations. *J. Clim.* 4, 517–528. doi:10.1175/1520-0442(1991)004<0517:TPATPA>2.0.CO;2

- Li, C., and Mu, M. (2000). Relationship between East Asian winter monsoon, warm pool situation and ENSO cycle. *Chin. Sci. Bull.* 45, 1448. doi:10.1007/BF02898885
- Liu, Y. M., Wu, G. X., Liu, H., and Ping, L. (1999). The effect of spatially nonuniform heating on the formation and variation of subtropical high part III: condensation heating and south Asia high and western pacific subtropical high. *Acta Oceanol. Sin.* 57 (5), 525–538.
- L'Heureux, M. L., Tippett, M. K., and Barnston, A. G. (2015). Characterizing ENSO coupled variability and its impact on north American seasonal precipitation and temperature. *J. Clim.* 28, 4231–4245. doi:10.1175/JCLI-D-14-00508.1
- Lorenz, E. N. (1956). Empirical orthogonal functions and statistical weather prediction. Massachusetts Institute of Technology Dept. of Meteorology Statistical Forecast Project Rep. 1.49 pp.
- Ma, X., Chang, P., Saravanan, R., Montuoro, R., Hsieh, J. S., Wu, D., et al. (2015). Distant influence of Kuroshio Eddies on North Pacific weather patterns? *Sci. Rep.* 5, 17785. doi:10.1038/srep17785
- McAfee, S. A., and Russell, J. L. (2008). Northern annular mode impact on spring climate in the western United States. *Geophys. Res. Lett.* 35, L17701. doi:10.1029/2008GL034828
- Mei, S. L., Min, J. Z., and Sun, Z. B. (2006). Relationships of Kuroshio SSTA and tropical pacific wind field as well as ENSO. *J. Nanjing Inst. Meteorol.* 29 (3), 385–389. doi:10.1016/S1003-6326(06)60040-X
- Minobe, S., Kuwano-Yoshida, A., Komori, N., Xie, S. P., and Small, R. J. (2008). Influence of the Gulf Stream on the troposphere. *Nature* 452, 206–209. doi:10.1038/nature06690
- Moteki, Q., and Manda, A. (2013). Seasonal migration of the Baiu Frontal Zone over the East China Sea surface temperature effect. *SOLA* 9, 19–22. doi:10.2151/sola.2013-005
- Mundhenk, B. D., Barnes, E. A., Maloney, E. D., and Baggett, C. F. (2018). Skillful empirical subseasonal prediction of landfalling atmospheric river activity using the madden–julian oscillation and quasi-biennial oscillation. *npj Clim. Atmos. Sci.* 2018, 20177. doi:10.1038/s41612-017-0008-2
- Nonaka, M., and Xie, S. (2003). Covariations of sea surface temperature and wind over the Kuroshio and its extension: evidence for ocean-to-atmosphere feedback. *J. Clim.* 16, 1404–1413. doi:10.1175/1520-0442(2003)16<1404:COSSTA>2.0.CO;2
- Payne, A. E., Demory, M., Leung, L. R., Ramos, A. M., Shields, C. A., Rutz, J. J., et al. (2020). Responses and impacts of atmospheric rivers to climate change. *Nat. Rev. Earth. Environl.* 1, 143–157. doi:10.1038/s43017-020-0030-5
- Seager, R., and Hoerling, M. (2012). Atmosphere and ocean origins of north american droughts. *J. Clim.* 27 (12), 4581–4606. doi:10.1175/JCLI-D-13-00329.1
- Simmons, A. J., and Hoskins, B. J. (1978). The life cycles of some nonlinear baroclinic waves. *J. Atmos. Sci.* 35 (3), 414–432. doi:10.1175/1520-0469(1978)035<0414:TLCOSN>2.0.CO;2
- Swain, D. L., Horton, D. E., Singh, D., and Diffenbaugh, N. S. (2016). Trends in atmospheric patterns conducive to seasonal precipitation and temperature extremes in California. *Sci. Adv.* 2 (4), e1501344. doi:10.1126/sciadv.1501344
- Taguchi, B., Nakamura, H., Nonaka, M., and Xie, S. P. (2009). Influences of the kuroshio/oyashio extensions on air-sea heat exchanges and storm-track activity as revealed in regional atmospheric model simulations for the 2003/04 cold season. *J. Clim.* 22 (24) 6536–6560. doi:10.1175/2009JCLI2910.1
- Takaya, K., and Nakamura, H. (2001). A formulation of a phase-independent wave-activity flux for stationary and migratory quasigeostrophic eddies on a zonally varying basic flow. *J. Atmos. Sci.* 58 (6) 608–627. doi:10.1175/1520-0469(2001)058<0608:AFOAPI>2.0.CO;2
- Thompson, D. W. J., and Wallace, J. M. (2001). Regional climate impacts of the northern hemisphere annular mode. *Science* 293 (5527), 85–89. doi:10.1126/science.1058958
- Thompson, D. W. J., and Wallace, J. M. (2000). Annular modes in the extratropical circulation. Part 1: month-to-month variability. *J. Clim.* 13 (5), 1000–1016. doi:10.1175/1520-0442(2000)013<1000:0CO;2
- Trenberth, K. E., Branstator, G. W., Karoly, D., Kumar, A., Lau, N.-C., and Ropelewski, C. (1998). Progress during TOGA in understanding and modeling global teleconnections associated with tropical sea surface temperatures. *J. Geophys. Res.* 103, 14 291–14 324. doi:10.1029/97JC01444
- Wallace, J. M., and Gutzler, D. S. (1981). Teleconnections in the geopotential height field during the Northern Hemisphere winter. *Mon. Weather Rev.* 109, 784–812. doi:10.1175/1520-0493(1981)109<0784:TITGHF>2.0.CO;2
- Wang, B., and LinHo (2002). Rainy season of the Asian–Pacific summer monsoon. *J. Clim.* 15 (4), 386–398. doi:10.1175/1520-0442(2002)015<0386:RSOTAP>2.0.CO;2
- Wu, G., Guan, Y., Liu, Y., Yan, J., and Mao, J. (2008). Modulation of land-sea distribution on air-sea interaction and formation of subtropical anticyclones. *Chin. J. Atmos. Sci.* 32 (4), 720–740. doi:10.3724/SP.J.1148.2008.00288
- Wu, G. X., Liu, Y. M., and Liu, P. (1999). The effect of spatially nonuniform heating on the formation and variation of subtropical high I: scale analysis. *Acta Meteor. Sinica* 57 (3), 257–263. doi:10.11676/qxxb1999.025
- Yanai, M., Esbensen, S., and Chu, J. H. (1973). Determination of bulk properties of tropical cloud clusters from large-scale heat and moisture budgets. *J. Atmos. Sci.* 30, 611–627. doi:10.1175/1520-0469(1973)030<0611:DOBPOT>2.0.CO;2
- Yu, G. C., Chen, W., Xu, P. Q., and Ma, J. (2015). Mechanistic analysis of the influence of the latent heat associated with the Kuroshio Current on Chinese rainfall anomalies in spring. *Clim. Environ. Res.* 20 (5), 600–610. doi:10.3878/j.issn.1006-9585.2015.15050
- Yu, L., Jin, X., and Weller, R. A. (2008). OAFlux Project Technical Report No.: OA-2008-01. Multidecade global flux datasets from the objectively analyzed air-sea fluxes (OAFlux) project: latent and sensible heat fluxes, ocean evaporation, and related surface meteorological variables. Woods Hole, MA: Woods Hole Oceanographic Institution, 64.
- Zhang, L., Xu, H., Shi, N., and Deng, J. (2017). Responses of the East Asian jet stream to the North Pacific subtropical front in spring. *Adv. Atmos. Sci.* 34 (2), 144–156. doi:10.1007/s00376-016-6026-x
- Zhang, Q. L., Hou, Y. J., and Yan, T. Z. (2012). Inter-annual and inter-decadal variability of Kuroshio heat transport in the East China Sea. *Int. J. Climatol.* 32, 481–488. doi:10.1002/joc.2295
- Zhao, X., Xu, H. M., Xu, M. M., and Deng, J. C. (2015). Spring atmospheric heat source over the East China Sea Kuroshio and its impact on precipitation in Eastern China. *Acta Oceanol. Sin.* 73 (2), 263–275. doi:10.11676/qxxb2015.013
- Zhu, Y., and Newell, R. E. (1994). Atmospheric rivers and bombs. *Geophys. Res. Lett.* 21 (18), 1999–2002. doi:10.1029/94GL01710
- Zhu, Z., and Li, T. (2016). A new paradigm for the continental united states summer rainfall variability: asia-north america teleconnection. *J. Clim.* 29 (20) 7313–7327. doi:10.1175/JCLI-D-16-0137.1
- Zhun, Y. F., and Chen, L. X. (2002). The relationship between the Asian/Australian monsoon and ENSO on a Quasi-Four-Year Scale. *Adv. Atmos. Sci.* 19, 727–739. doi:10.1007/s00376-002-0012-1

Conflict of Interest: The authors declare that the research was conducted in the absence of any commercial or financial relationships that could be construed as a potential conflict of interest.

Copyright © 2021 Long, Liu, Liu and Xu. This is an open-access article distributed under the terms of the Creative Commons Attribution License (CC BY). The use, distribution or reproduction in other forums is permitted, provided the original author(s) and the copyright owner(s) are credited and that the original publication in this journal is cited, in accordance with accepted academic practice. No use, distribution or reproduction is permitted which does not comply with these terms.